Electrochemical Investigations on the Effect of Dispersoid in PVA Based Solid Polymer Electrolytes

S. Rajendran,[1] M. Sivakumar,[2] R. Subadevi,[1] N.-L. Wu,[2] J.-Y. Lee[3]

[1]Department of Physics, Alagappa University, Karaikudi 630 003, India
[2]Department of Chemical Engineering, National Taiwan University, Taipei 106, Taiwan, Republic of China
[3]Department of Materials Science and Engineering, Korea Advanced Institute of Science and Technology (KAIST), Taejon 305-702, South Korea

ABSTRACT: Various compositions of TiO_2 dispersed PVA-PMMA-LiBF$_4$-EC based electrolytes were prepared using solution casting technique. The prepared electrolytes were characterized using AC impedance, XRD, SEM, FTIR, etc. The ionic conductivity value is increased with the increase in filler content (up to 8 wt %) and then decreased with the increase in filler content. The results are described using Vogel–Tamman–Fulcher theory. The thermal and transport properties of the electrolyte exhibiting maximum conductivity have also been studied. © 2006 Wiley Periodicals, Inc. J Appl Polym Sci 103: 3950–3956, 2007

Key words: composite; poly(vinyl alcohol); ionic conductivity; XRD; FTIR

INTRODUCTION

A lot of research into solid polymer electrolytes for use in lithium (Li)-ion batteries has been carried out. Ion conducting composites are a versatile class of solid electrolytes.[1–5] For polymer electrolytes to be of practical use, Li-ion mobility must be high enough to enable useful rate capabilities in Li batteries. In the search for new polymer electrolyte systems, the addition of inert oxide filler in continuation of salts and plasticizers with the polymer matrix has been hotly pursued in the past few years.[6–8] Ceramics are crystalline inorganic materials that are generally stable up to high temperature and remain chemically unreactive. The idea is that these fillers may act as solid plasticizers, capable of enhancing the composite polymer electrolyte's transport properties without affecting its mechanical and interfacial stability.[9] The dispersion of ceramic fillers in polymer electrolytes to improve their mechanical strength was first suggested by Weston and Steele[10]; also since then, a number of ceramic additives have been reported in literature.[11–13]

The addition of ceramic fillers increases the conductivity, which has been found to depend upon the concentration and particle size of the inert phase matrix, and the resulting electrolytes are known as composite solid electrolytes. The increase in conductivity is generally explained[1,8–13] to be either due to the formation of a new kinetic path via a thin interface layer along the interface itself, or due to a concentration enhancement due to space charges in the subinterface region. Thus, a combination of desirable characteristics makes these materials highly promising candidates for use in rechargeable lithium batteries.

PVA is a polymer that can be blended with ceramics into thin and uniform slurries. This provides a new route for the dispersion of selected ceramic powders in the polymer mass of desired compositions to obtain ceramic composites showing consistent improvements in both interfacial and transport properties. With a view to obtaining high ionic conductivity, an attempt has made to prepare composite electrolyte by dispersing TiO_2 in PVA-PMMA-LiBF$_4$-EC system. The choice of PVA and PMMA polymeric blend materials has already been reported by Singh and Singh (who used ultrasonic and viscometric techniques),[14] as they have good compatible nature in solution, and also been reported in our previous works.[15,16] They were characterized for their crystalline structure, surface morphology, conductivity, thermal stability, etc., and the results are discussed in detail.

EXPERIMENTAL

The various compositions of TiO_2, (size of <5 μm, from Aldrich, USA) such as 4, 8, 12, and 16 wt %, were dispersed in PVA(15%)-PMMA(10%)-LiBF$_4$ (8%)-EC(67%) system. The electrolyte films were prepared
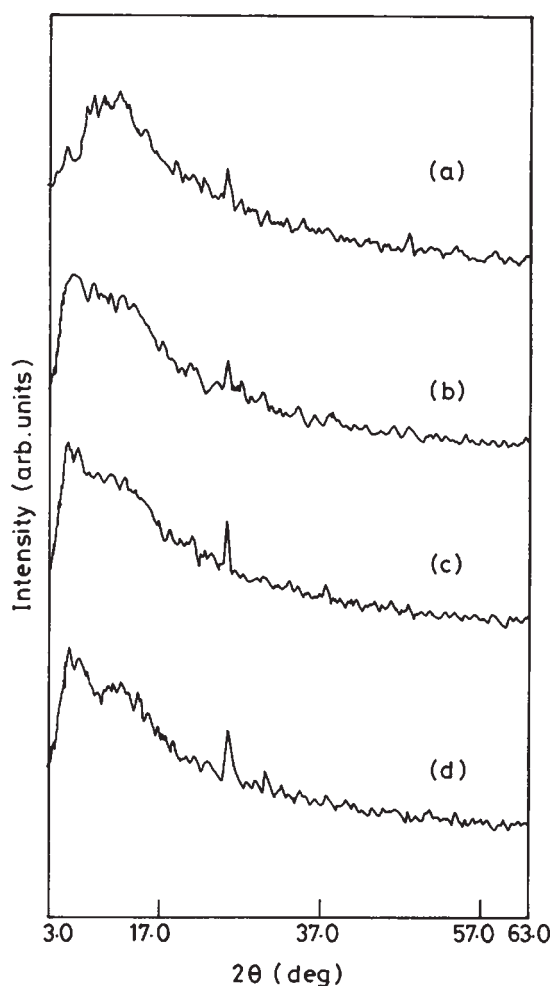
Figure 1 X-ray diffractions patterns of PVA(15)-PMMA(10)-LiBF$_4$(8)-EC(67)-TiO$_2$(X) systems where X = (a) 4, (b) 8, (c) 12, and (d) 16 wt %.

using solvent casting technique,[15–17] since it reduces the energy for melting. After dispersing the TiO$_2$ into the slurries, the mixture was stirred for 2 h. The resulting slurries were cast on Teflon sheets and glass plates. The samples were kept under vacuum at 75°C for 5–7 h to get rid of traces of solvent.

Conductivity measurements were carried out by sandwiching the electrolytes between two stainless steel (SS) electrodes in a home made conductivity jig, and AC impedance measurements were performed using Keithley LCZ meter (model 3330) in the temperature range of 302–373 K (with a signal amplitude of 10 mV and the frequency range was 40 Hz–100 kHz). The lithium ion transference number measurements were carried out for the Li/SPE/Li cells by applying a DC voltage of 10 mV across the sample and the current was monitored with respect to time using ECO CHEMIE PGSTAT 30.

The X-ray diffraction analysis was carried out using JEOL JDX 8030 X-ray diffractometer. FTIR studies were performed for the prepared electrolytes

in the range of 4000–400 cm^{-1} using a PerkinElmer 577 IR spectrophotometer. Thermal history of the samples was studied using thermogravimetric/differential thermal analysis (TG/DTA) apparatus (model STA 1500, PL Thermal Sciences, UK) at a heat rate of 10°C/min up to 700°C. To investigate the cyclability and reversibility of the electrolytes, cyclic voltammetric (CV) studies were performed using EG and G Impedance Analyzer model 6310. Surface morphology of the electrolytes was evaluated by scanning electron microscopic (SEM) studies using S3000H scanning electron microscope.

RESULTS AND DISCUSSIONS

X-ray diffraction analysis

To examine the crystalline structure of electrolyte films due to the influence of addition of TiO$_2$ in the PVA(15)-PMMA(10)-LiBF$_4$(8)-EC(67) system, X-ray diffraction studies were performed. Figure 1(a–d) show the X-ray diffraction patterns of 4, 8, 12, and 16 wt % of TiO$_2$ based complexes (films M2, M3, M4, and M5) respectively.

The only peaks observed (2θ = 25.3° and 48.0°) are due to TiO$_2$. No peaks pertaining to pure PVA and LiBF$_4$ are present in the complexes, revealing the complex formation in the polymer–salt matrices. In addition to that, the plasticizer EC also provides more amorphous phase and current carriers in the polymer–salt matrix.[18] The degree of crystallinity has been estimated as 1.13, 0.95, 1.23, and 1.35% for the films M2, M3, M4, and M5 respectively. The maximum conductivity value of the electrolyte M3 is in accordance with the lowest degree of crystallinity (0.95%) among the others. Even though the degree of crystallinity (0.77%) of ceramic-free complex is lower than that of film M3, it exhibits minimum conductivity when compared with the ceramic filler based complexes. This may be due to the free complex in the amorphous phases and ionic paths created in the polymer matrices. Thus, the complexation in the polymer matrices has been confirmed from the above-mentioned analysis.

FTIR

The typical FTIR spectrum of 8 wt % of TiO$_2$ based PVA(15)-PMMA(10)-LiBF$_4$(8)-EC(67) system is shown in Figure 2. The main feature of alcohols and phenols is the appearance of OH (hydroxyl) vibrational band at 3575 cm^{-1} in the range 3600–3400 cm^{-1}. This band of PVA gets displaced toward the lower wavenumber and appeared as broad hydroxyl band in the complex. The absorption bands at 1726, 1410, 1260, and 851 cm^{-1} are assigned to C=O stretching of unhydrolyzed acetate portions, weak OH bending
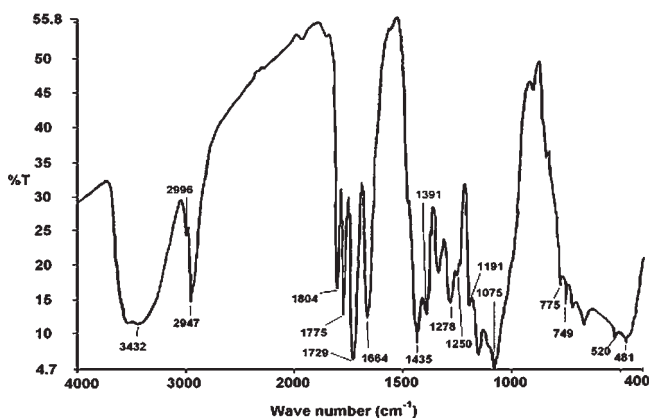
Figure 2 FTIR spectra of 8 wt % of TiO₂ based PVA(15)-PMMA(10)-LiBF₄(8)-EC(67) based complex.

deformation, C—O bend deformation, and CH rocking mode of PVA. These bands are shifted to 1729, 1391, 1247, and 844 cm^{-1} in the complex. The C—C stretching frequency of secondary alcohols of PVA at 1100 cm^{-1} is displaced to 1075 cm^{-1} in the film M3. An asymmetric CH₂ stretching and CH bend of CH₂ attributed to PVA at 2925 and 1465 cm^{-1} are found to be absent in the complex.

The vibrational peak at 2954 cm^{-1} is assigned to CH₃ asymmetric stretching of PMMA, which is shifted to 2947 cm^{-1} in the complex. The C=O stretching of PMMA at 1736 cm^{-1} disappeared in the complexes. The characteristic vibrational peaks at 3010, 1452, 1389, 1280, 1173, and 750 cm^{-1} are assigned to O—CH₂ asymmetric stretching, CH₃ asymmetric bend, O—CH₃ deformation, C—O stretching, CH₂ twisting, and rocking modes of PMMA. These vibrational peaks are shifted to 2996, 1435, 1391, 1278, 1191, and 749 cm^{-1} in the complex. The CH₂ scissoring (1483 cm^{-1}), wagging mode (947 cm^{-1}), and C—O—C stretching (874 cm^{-1}) of PMMA are found to be absent in the complex.

The characteristic vibrational peak of LiBF₄ at 510 cm^{-1} is assigned to BF₄$^{-}$, which is shifted to 520 cm^{-1} in the complex. This provides information about the specific interactions in the polymer–salt matrices. The vibrational frequency appearing at 1810 cm^{-1}is assigned to $\nu_{C=O}$ region of skeletal breathing of EC,[19] which is shifted to 1804 cm^{-1} in the complex. One of the important bands in $\nu_{C=O}$ region is due to Fermi resonance of skeletal breathing around 1788 cm^{-1}, which is shifted to 1775 cm^{-1} in the complex containing TiO₂. This downward shift of $\nu_{C=O}$ region 1775 cm^{-1} indicates the interaction of EC with LiBF₄ salt on complexation. The absorption peak at 770 cm^{-1}, attributed to CH₂ group of EC, is shifted to 775 cm^{-1} in the complex. The absorption peaks at 3891, 3810, 3788, 3698, and 3660 cm^{-1} of PVA, 3446, 1508, 1056, and 990 cm^{-1} of PMMA, 3563.1305, and 1056 cm^{-1} of LiBF₄, and 3566, 2775, 2659, and 2550 cm^{-1} of EC are absent in the complexes. From

the above-mentioned analysis, complex formation in the polymer matrices has been corroborated.

Conductivity studies

The complex impedance plot of 8 wt % of TiO₂ based PVA(15)-PMMA(10)-LiBF₄(8)-EC(67) system is shown in Figure 3, in the temperature range of 302–373 K. Theoretically, for the symmetric cell containing SS electrodes, the impedance spectrum appears as two semicircles; one is at higher frequencies corresponding to the bulk electrolyte impedance and the other at lower frequencies related to the interfacial impedance. In the present case, the elimination of high frequency semicircular portion suggests that the current carriers are the ions and also the total conductivity is mainly due to the result of ion conduction. This phenomenon is also found in many plasticized systems in the literature.[20]

The ionic conductivity values of the electrolytes have been determined and listed in Table I , in the temperature range of 302–373 K. The maximum conductivity value 2.3×10^{-3} S cm^{-1} is obtained for 8 wt % of TiO₂ based complex (film M3). PVA and PMMA blend without plasticizer exhibits a conductivity value of about 2.80×10^{-5} S cm^{-1}.[21] After
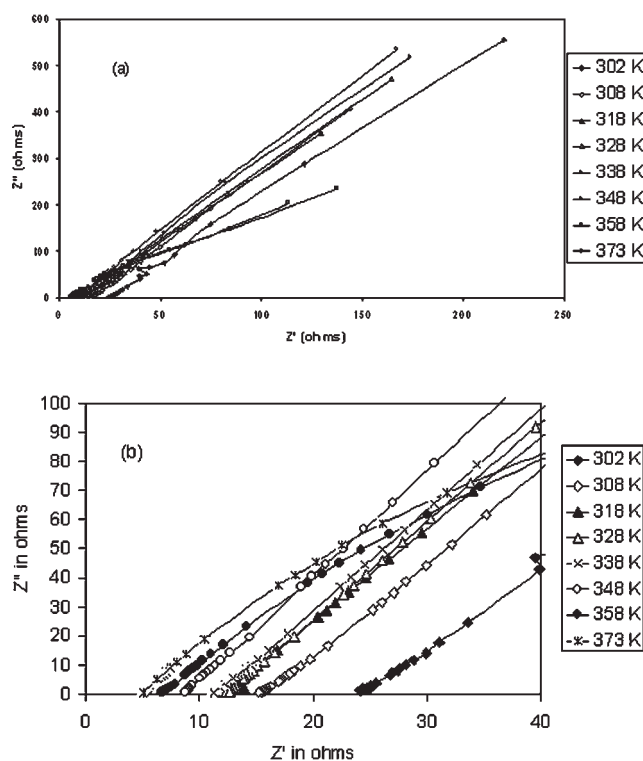

Figure 3 (a) Complex impedance plot of 8 wt % of TiO₂ based PVA(15)-PMMA(10)-LiBF₄(8)-EC(67) system in the temperature range of 302–373 K. (b) Enlarged portion of the complex impedance plot of the above complex in the higher frequency range.

TABLE I
Ionic Conductivity Values of 0, 4, 8, 12, and 16 wt % of TiO$_2$-Based PVA(15)-PMMA(10)-LiBF$_4$(8)-EC(67) System at 302 K

	σ Values of PVA(15)-PMMA(10)-LiBF$_4$(8)-EC(67)-TiO$_2$(X) system (10^{-3} S cm^{-1})							
X	302 K	308 K	318 K	328 K	338 K	348 K	358 K	373 K
0 wt % (M1)	1.289	2.323	3.285	4.502	5.893	7.547	8.789	9.038
4 wt % (M2)	1.767	2.352	3.515	4.625	6.050	7.670	9.366	11.106
8 wt % (M3)	2.30	3.357	4.666	6.160	8.915	13.05	19.230	28.805
12 wt % (M4)	1.982	2.392	4.095	5.058	6.514	9.424	11.001	13.695
16 wt % (M5)	1.787	2.368	3.591	4.997	6.387	8.417	10.493	12.001

incorporating the plasticizer with a proper concentration of LiBF$_4$ (i.e., 8 wt %), the conductivity is improved by two orders of magnitude (1.28 × 10^{-3} S cm^{-1}).[16] Although, TiO$_2$ itself facilitates higher ionic conduction and mechanical strength for the electrolyte, the plasticizer EC provides more flexibility with greater conducting pathways for mobile species because of its high dielectric constant such as 89.6 at 40°C. Also this present work has been discussed in the view point of improved performance in the parent blend electrolyte, viz. PVA(15)-PMMA(10)-LiBF$_4$(8)-EC(67) system. Actually, the hydroxyl group in PVA also assists in hydrogen bonding in the polymer network and it has been evidenced from the FTIR studies.

The incorporation of ceramic fillers enhances free volume, which leads to higher salt dissociation, and also the defects introduced while dispersing the composite particles. A new transport mechanism develops because of an interaction of the polymer and ceramic phases. This transport mechanism provides a path for the conduction of lithium ions.[22–24] Therefore an appreciable enhancement in the conductivity has been obtained for the heterogeneous electrolyte. The improvement in conductivity can also be attributed to the ceramic particles, acting as a nucleation centers for the formation of minute crystallites and the ceramic particles aiding in the formation of amorphous phases in the polymer electrolyte. The maximum conductivity is obtained for 8 wt % TiO$_2$ based complex (film M3). With further raise in TiO$_2$ content, the conductivity value falls down. Similar observations were already made by Qian et al.[25] for PEO-based composite polymer electrolytes. This behavior is a direct consequence of high concentrations of TiO$_2$, which leads to well-defined crystallite regions, and the TiO$_2$ particles tend to impede ionic movement by acting as mere insulators.

Figure 4 shows the temperature dependence of ionic conductivity plots for 0, 4, 8, 12, and 16 wt % of TiO$_2$ based PVA(15)-PMMA(10)-LiBF$_4$(8)-EC(67) system. For all the complexes, conductivity increases with the increase in temperature and this can be rationalized by recognizing the free volume model.[13] The curvature of the plots indicates that ionic con-
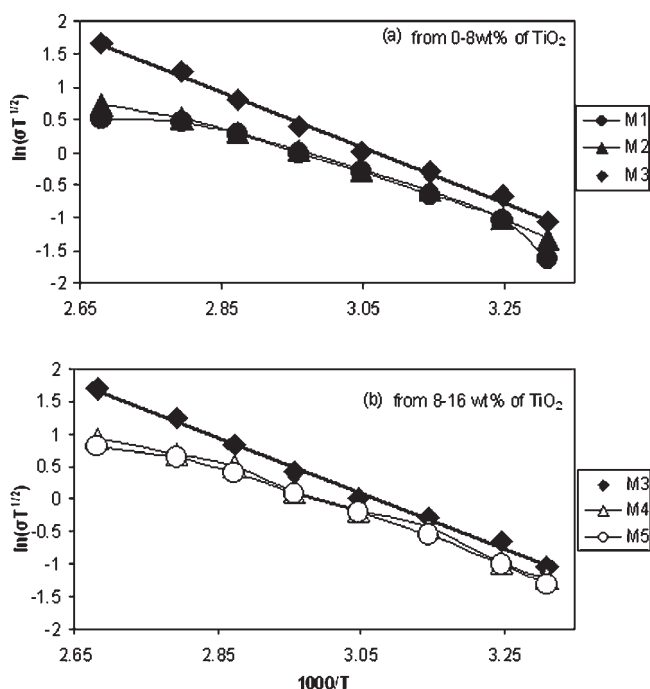

Figure 4 Temperature dependent plots of (a) 0, 4, and 8 wt % and (b) 8, 12, and 16 wt % of TiO$_2$ based PVA(15)-PMMA(10)-LiBF$_4$(8)-EC(67) system.
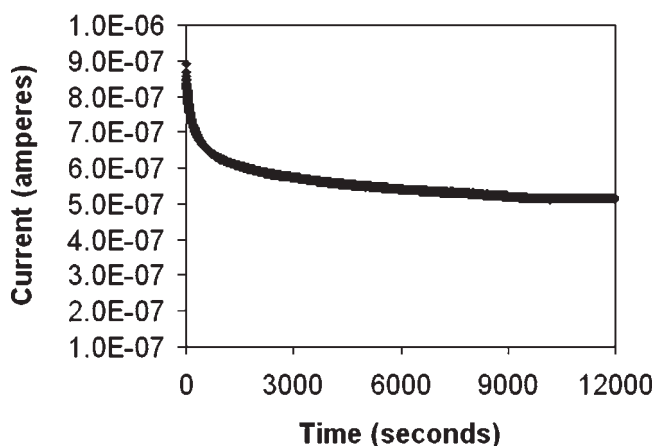

Figure 5 Polarization current versus time plot for 8 wt % of TiO$_2$ based complex at 302 K.
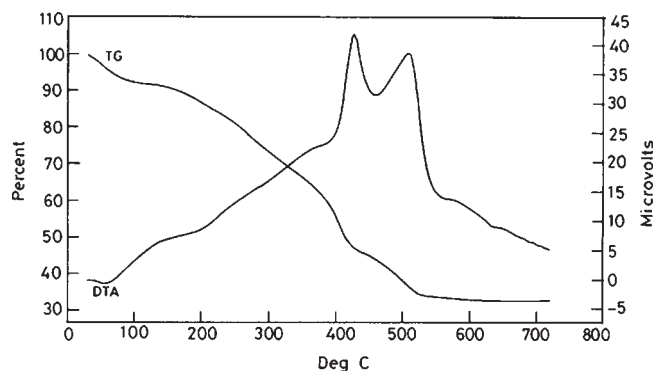
Figure 6 TG/DTA curve of PVA(15)-PMMA(10)-LiBF$_4$(8)-EC(67)-8 wt % TiO$_2$ system.

duction probably obeys Vogel–Tamman–Fulcher (VTF) relation, which describes that the ion transport in polymer electrolytes is dependent on polymer segmental motion. Thus, the result may be effectively represented by the empirical VTF equation.[26–28]

$$\sigma = A\,T^{-1/2}\,\exp(-E_a/k(T-T_0))$$

where A is the fitting constant proportional to the number of charge carriers, E_a is the activation energy of ion transport associated with the configurational entropy of the polymer chains, k is the Boltzmann constant, and T is the temperature and T_0 is the reference temperature approximately equal to the glass transition temperature. Non linearity of the plots (slightly exempted for the film M3) suggests that the ion transport in the polymer electrolytes takes place by the polymer segmental motion. Only film M3 seems to obey the VTF relation and probably fits the linear line. The activation energy and fitting constant A are estimated as 0.37 eV and 4.88×10^5 respectively. For the complex without TiO$_2$, the curvature of the plot is more and it is reduced by adding the TiO$_2$ into it. This reaches to a reasonably linear line for the complex containing 8 wt % of TiO$_2$, after which the curvature is again increased with further addition of TiO$_2$. Adding TiO$_2$ in the parent system provides the conducting pathway for the mobile species and enhances the ion hopping between the coordinating sites and accompanied by local structural relaxation and segmental motion of the polymer. It is observed that for film M3, the sufficient disorder or number of vacancies for the ions to hopping/jumping from one site to other is more among the other complexes studied, which is supported by the results of SEM studies. Further addition of TiO$_2$ minimized the dipoles in the polymer matrix and maximized the coordination effect between the ceramic particles and merely impedes the mobility of ions. Thus the results may be described by the VTF relation, which describes the transport properties in a viscous matrix. The curvature of the plots suggests

that the ion transport in the polymer electrolytes is associated with the polymer segmental motion. Also it indicates that the conductivity of polymer electrolyte is thermally activated.

Transference number measurements

The lithium ion transference number of the electrolyte sample that exhibits maximum conductivity was determined for the symmetric cell with lithium metal (Fig. 5) at 302 K. It was estimated as 0.51; it is due to the reaction between lithium metal and hydroxyl group in PVA and also due to the aprotic solvent EC serving as a plasticizer. This value is quite obvious to use in the lithium battery application in accordance with Heitner.[29]

TG/DTA analysis

TG/DTA curve of 8 wt % of TiO$_2$ based PVA(15)-PMMA(10)-LiBF$_4$(8)-EC(67) system is shown in Figure 6. The host polymer (PVA) is known to decompose in two stages and it is thermally stable up to 265°C.[30] The initial transition takes place before 100°C, which may be due to the moisture. The actual decomposition of the film takes place above165°C with weight loss of about 9%; then, there is a gradual weight loss of 30% up to 395°C. After that, there is a rapid weight loss of 53% up to 420°C. The complete decomposition occurred between 450 and 535°C with the corresponding weight losses of about 55–68%. No effort has been made to confirm the decomposition products, as it is well known that the decomposition leads to evolution of alkanes, alkenes, ketones, etc., and also acetaldehyde and acetic acid in case of pure PVA.[31] Therefore, it is confirmed that most of the residue in the sample could also be from unhydrolyzed acetate portion of PVA. In the DTA curve, there are two large exothermic peaks at 425 and 507°C concurrent with the
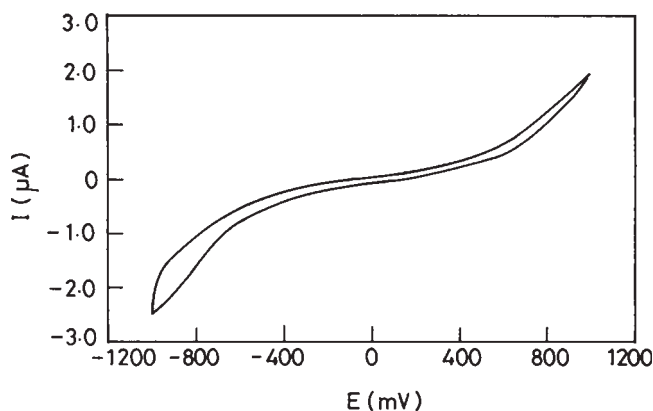

Figure 7 Cyclic voltammogram of PVA(15)-PMMA(10)-LiBF$_4$(8)-EC(67)-8 wt % TiO$_2$ system with the SS electrode; scan rate 5 mV/s.
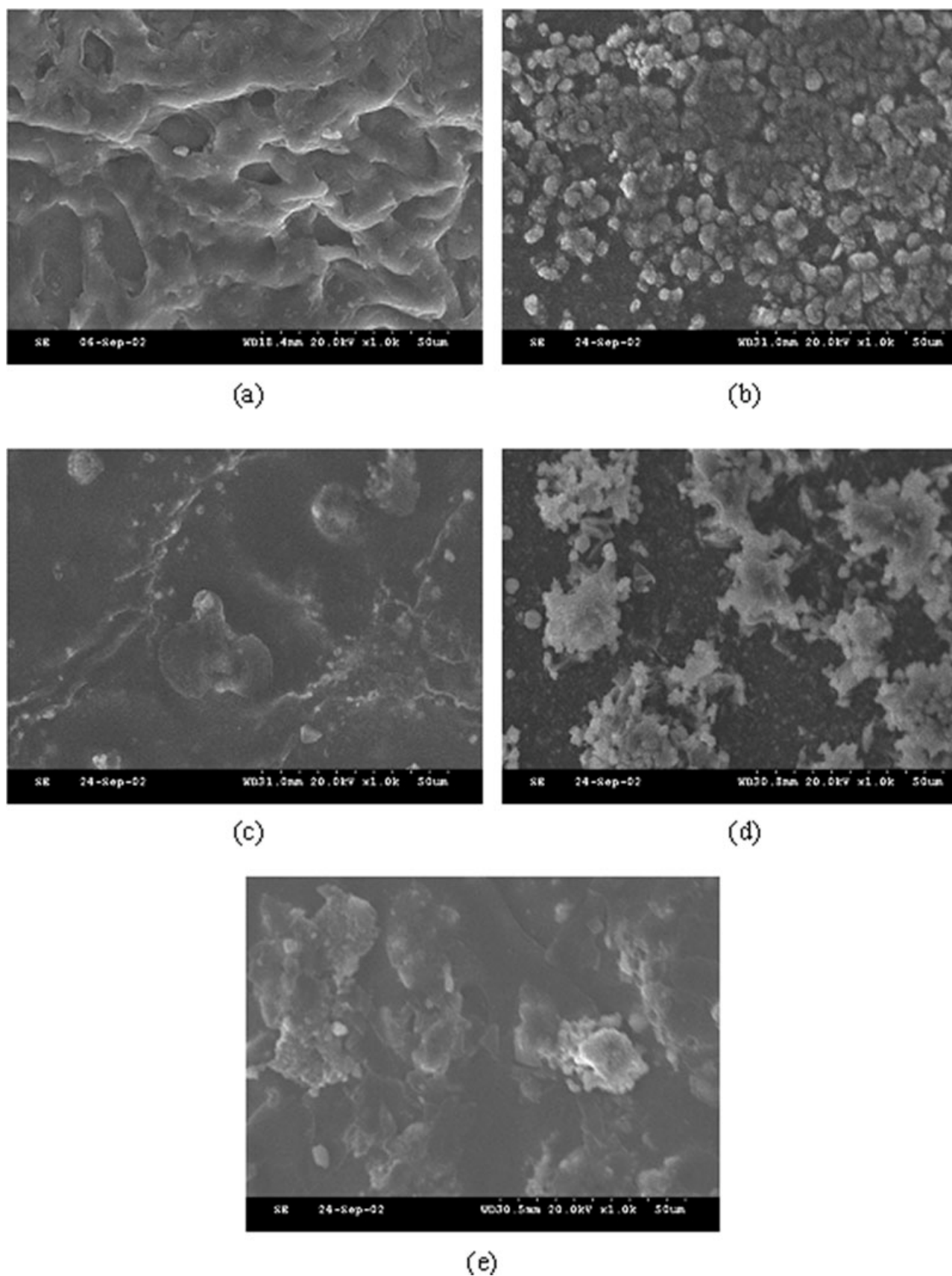
Figure 8 SEM images of PVA(15)-PMMA(10)-LiBF$_4$(8)-EC(67)-TiO$_2$(X) systems, where X = (a) 0, (b) 4, (c) 8, (d) 12, and (e) 16 wt % with the magnification of (×1000).

weight losses. Hence from the thermogram, it is concluded that the thermal stability of the electrolyte film (M3) is affected by the addition of TiO$_2$ when compared with the parent blend electrolyte[15] and also it is thermally stable up to 165°C.

Cyclic voltammetry

Figure 7 represents the cyclic voltammogram of 8 wt % of TiO$_2$ based PVA(15)-PMMA(10)-LiBF$_4$(8)-EC(67) complex. The cyclic voltammetry has been performed for the SS/polymer electrolyte/SS cell couple with a scan rate of 5 mV/s. CV studies employing SS electrodes have already been carried out by Kumar and Munichandraiah[32] for the polymer electrolytes based on PVdF and PMMA. The following points are observed from the cyclic voltammogram.

The electrochemical window has been obtained from −1000 mV to +1000 mV for PVA-PMMA-LiBF$_4$-EC-TiO$_2$(8 wt %) polymer composite electrolyte. The cathodic and anodic peaks are not observed, which suggests negligible interaction of Lithium in the polymer electrolyte with the SS electrodes. This voltammogram strongly indicates that the polymer electrolyte has excellent reversibility and cyclability.

SEM studies

Figure 8(a–e) shows the scanning electron micrographs of 0, 4, 8, 12, and 16 wt % of TiO$_2$ based PVA(15)-PMMA(10)-LiBF$_4$(8)-EC(67) system. The addition of ceramic filler provides sponge-like spherulites that favor the fast ion transport. The 8 wt % of TiO$_2$ based complex [Fig. 8(c)] shows that the ceramic particles present in the sample are more dispersed when compared with others. Further addition of TiO$_2$ causes the well-defined crystallite regions and the ceramic particles tend to impede ionic movement by acting as mere insulator, and hence the decrease in conductivity.

CONCLUSIONS

1. PVA (15)-PMMA(10)-LiBF$_4$(8)-EC(67) hybrid solid polymer electrolytes with 4, 8, 12, and 16 wt % of TiO$_2$ have been prepared using the solvent casting technique. Complexation has been vividly confirmed by FTIR analysis.
2. The maximum conductivity value (2.3 × 10^{-3} S cm^{-1} at 302 K) has been obtained for 8 wt % of TiO$_2$ based complex. The conductivity values of the electrolytes first increase and then decrease with increase in TiO$_2$. The oxide filler provides additional pathways for transport inside the matrix and acts as a ''solid plasticizer''.
3. From the TG/DTA analysis, it is observed that the 8 wt % of TiO$_2$ based PVA(15)-PMMA(10)-LiBF$_4$(8)-EC(67) system is thermally stable up to 165°C.
4. The electrolyte having maximum conductivity possesses reasonable transference number and appreciable cyclability and reversibility.

Hence this electrolyte can be used as a potential candidate in lithium battery fabrication.

References

1. Liang, C. C. J Electrochem Soc 1973, 120, 1289.
2. Shahi, K.; Wagner, J. B. Appl Phys Lett 1980, 37, 757.
3. Shahi, K.; Wagner, J. B. J Electrochem Soc 1981, 128, 6.
4. Shahi, K.; Wagner, J. B. J Phys Chem Solids 1982, 43, 713.
5. Maier, J. J. Prog Solid State Chem 1995, 23, 171.
6. Srivastava, N.; Chandra, S. Phys Status Solidi A 1997, 163, 313.
7. Zalewska, A.; Wieczorek, W.; Przyluski, J. In 10th International Conference on Solid State Ionics, Singapore, 1995; p 225. Extended abstracts.
8. Agrawal, S. L.; Shukla, P. K.; Srivastava, P. K. Bull Electrochem 1996, 12, 727.
9. Croce, F.; Appetecchi, G. B.; Persi, L.; Scrosati, B. Nature 1998, 394, 456.
10. Weston, J. E.; Steele, B. C. H. Solid State Ionics 1982, 7, 75.
11. Wieczoreck, W.; Florjanezyk, Z.; Stevens, J. R. Electrochim Acta 1995, 40, 2251.
12. Choi, B.-K.; Shin, K.-H. Solid State Ionics 1996, 86–88, 303.
13. MacCallum, J. R.; Vincent, C. A., Eds. Polymer Electrolyte Reviews, Vols. 1 and 2; Elsevier: New York, 1987 and 1989.
14. Singh, Y. P.; Singh, R. P. Eur Polym J 1983, 19, 535.
15. Rajendran, S.; Sivakumar, M.; Subadevi, R. J Appl Polym Sci 2003, 90, 2794.
16. Rajendran, S.; Sivakumar, M.; Subadevi, R. J Power sources 2003, 124, 225.
17. Rajendran, S.; Sivakumar, M.; Subadevi, R. Solid State Ionics 2004, 167, 335.
18. Ramesh, S.; Arof, A. K. J Power Sources 2001, 99, 41.
19. Nyquist, R. A.; Settineri, S. E. Appl Spectros 1991, 45, 1991.
20. Song, J. Y.; Wang, Y. Y.; Wan, C. C. J Electrochem Soc 2000, 147, 3219.
21. Sivakumar, M.; Subadevi, R.; Rajendran, S.; Wu, N.-L.; Lee, J.-Y. Mater Chem Phys 2006, 97, 330.
22. Appetecchi, G. B.; Croce, F.; Persi, L.; Ronci, F.; Scrosati, B. Electrochim Acta 2000, 45, 1481.
23. Croce, F.; Persi, L.; Scrosati, B.; Serraino-Fiory, F.; Plichta, E.; Hendrickson, M. A. Electrochim Acta 2001, 46, 2457.
24. Kumar, B.; Scanlon, L. G. Solid State Ionics 1999, 124, 239.
25. Qian, X.; Gu, N.; Cheng, Z.; Yang, X.; Wang, E.; Dong, S. Electrochim Acta 2001, 46, 1829.
26. Vogel, H. Phys Z 1922, 22, 645.
27. Tamman, V. G.; Hesse, H. Z Anorg Allg Chem 1926, 19, 245.
28. Fulcher, G. S. J Am Ceram Soc 1925, 8, 339.
29. Heitner, K. L. J Power Sources 2000, 89, 128.
30. Mishra, R.; Rao, K. J. Eur Polym J 1999, 35, 1883.
31. Cardens, G.; Munoz, C.; Tagle, L. H. J Thermal Anal 1995, 44, 123.
32. Girish Kumar, G.; Munichandraiah, N. Electrochim Acta 2002, 47, 1013.